Electronic Supplementary Information

Near-infrared optically active $Cu_{2-x}S$ nanocrystals: sacrifice template-ligand exchange integration fabrication and chirality dependent autophagy effects

Yue Wang and Yunsheng Xia*

Key Laboratory of Functional Molecular Solids, Ministry of Education, College of Chemistry and Materials Science, Anhui Normal University, Wuhu 241000, China

1. Experimental section

1.1 Materials

Cuprous acetate (CH_3CO_2Cu), trioctylamine ($[CH_3(CH_2)_7]_3N$), oleic acid ($CH_3(CH_2)_7CH_2CH(CH_2)_7CO_2H$), n-hexane, ethanol, hydrogen peroxide (H_2O_2, 30 %), sodium hydroxide (NaOH), CH_3COOH (HAc), CH_3COONa (NaAc) and 3,3',5,5'-tetramethylbenzidine dihydrochloride (TMB) were purchased from Aladdin Chemistry. L-cysteine, D-cysteine were obtained from Alfa Aesar. Phosphate-buffered saline (PBS), Dulbecco's Modified Eagle Medium (DMEM), fetal bovine serum (FBS), 0.05% trypsin-EDTA and penicillin-streptomycin were provided from Gibco Invitrogen Co. (New York, USA). Cell counting kit-8 (CCK-8) and Reactive Oxygens Species assay kit (ROS assay kit) were purchased from Beyotime Biotechnology. Cyto-ID autophagy detection kit was obtained from Enzo Life Sciences, Inc. Live-dead cell staining kit (calcein-AM/PI double stain kit) was purchased from Shanghai Yeasen Biotechnologies Co., Ltd. All solutions were prepared with double deionized water.

1.2 Instruments

Extinction spectra and circular dichroism (CD) spectra were measured with a Hitachi U-2910 spectrophotometer and an Applied Photophysics Chirascan-plus CD spectropolarimeter (Leatherhead, UK), respectively. Transmission electron microscopy (TEM) photographs were taken with a Hitachi HT-7800 microscope at an accelerating voltage of 100 kV. High resolution (HR) TEM photographs were detected by a FEI Tecnai F20 transmission electron microscope at an acceleration voltage of 200 kV. Dynamic light scattering (DLS) analysis was performed on a Malvern ZS90 Zetasizer Nano instrument. Fourier transform infrared (FT-IR) spectra were measured by a PerkinElmer PE-983 FT-IR spectrophotometer. X-ray powder

diffraction (XRD) patterns were characterized with a Bruker D8 Advance X-ray diffractometer with Cu K_α radiation (λ = 0.15418 nm). X-ray photoelectron spectroscopy (XPS) was carried out with ESCALAB 250Xi. X-ray absorption near edge spectroscopy (XANES) measurements were conducted at beamline BL15U at Shanghai Synchrotron Radiation Facility (SSRF). Cellular viability experiments were analyzed with a Multiskan Sky microplate reader (Thermo Scientific, Waltham, MA). Photothermal irradiation were conducted by an 808 nm laser with 0.75 W cm^{-2} (CNI, China) and the temperature was measured by an infrared thermal imaging instrument (FLIR, A65). Automated inverted optical microscope (Olympus IX83, Japan). Fluorescent images of cells were taken by a confocal laser scanning fluorescence microscope (TCS SP8, Leica). Atomic absorption spectroscopy (AAS, Thermo Scientific FS95) was used to conduct cellular uptake analysis.

1.3 Synthesis of oleic acid capped Cu@$Cu_{2-x}O$ NCs

Oleic acid capped Cu@$Cu_{2-x}O$ NCs were synthesized by using the method previously reported by O'Brien et al.[1] First, a solution containing 4 mmol cuprous acetate, 4 mL of oleic acid and 15 mL of trioctylamine was pumped and inputted of argon three times by double row tube to remove dissolved oxygen. Then the solution was vigorously stirred and quickly heated under argon to 180 °C for 1 h. Second, the solution was heated further to 270 °C for 1 h before it was naturally cooled to room temperature. At last, the obtained Cu NCs were washed by ethanol three times and dispersed in n-hexane. It gradually produced a deep green solution which indicated Cu NCs were oxidized by oxygen in air.

2. Additional data

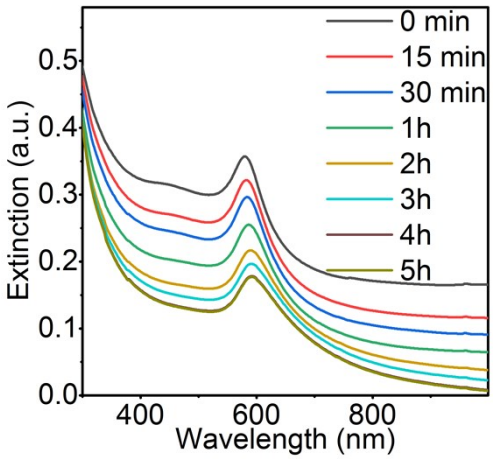

Fig. S1 The evolution of the LSPR extinction spectra of the oleic acid capped Cu NCs in air.

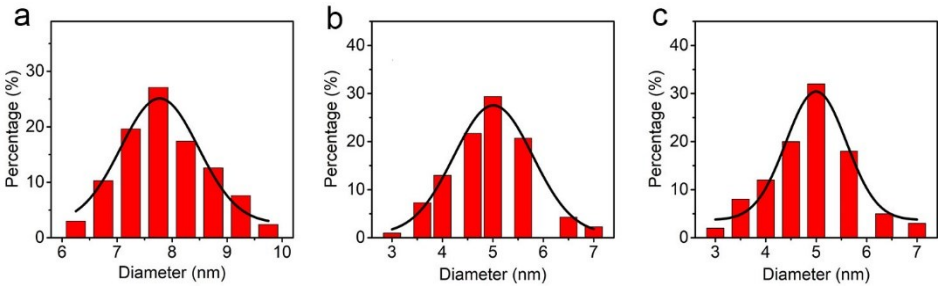

Fig. S2 Size distribution diagrams of the oleic acid capped Cu@$Cu_{2-x}O$ (a), D- (b) and L- $Cu_{2-x}S$ (c) NCs. The sizes of the three NCs are 7.96 ± 0.66, 4.84 ± 0.91 and 4.91 ± 0.73 nm, respectively (All the results are obtained by the statistics of 200 corresponding NCs, respectively).

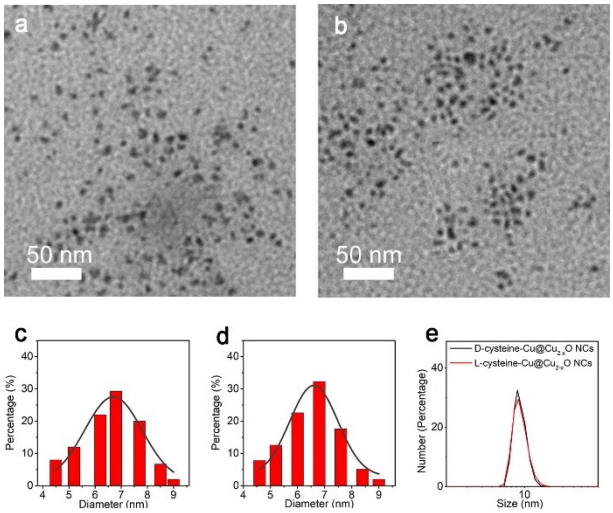

Fig. S3 TEM images of D- (a) and L-cysteine (b) modified Cu@$Cu_{2-x}O$ NCs, size distribution diagrams of D- (c) and L-cysteine (d) modified Cu@$Cu_{2-x}O$ NCs and DLS analysis (e) of D- and L-cysteine modified Cu@$Cu_{2-x}O$ NCs. The sizes of D- and L-cysteine modified Cu@$Cu_{2-x}O$ NCs are 6.82 ± 1.29 nm and 6.95 ± 1.25 nm, respectively. The hydrodynamic sizes of D- and L-cysteine modified Cu@$Cu_{2-x}O$ NCs are 8.22 and 8.46 nm, respectively. After phase transfer from n-hexane to water solution, both D- and L-cysteine modified Cu@$Cu_{2-x}O$ NCs are well dispersed, and they have almost completely identical morphology and size.

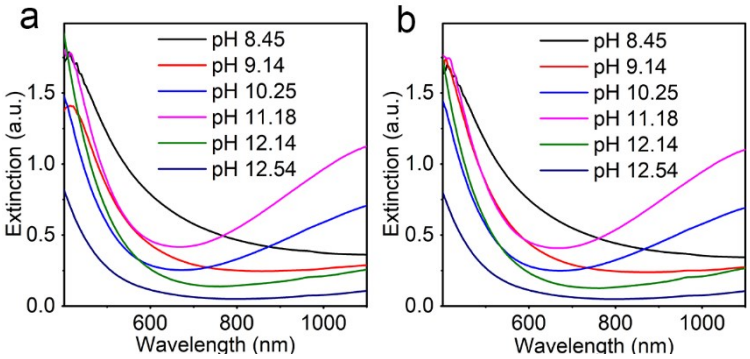

Fig. S4 The extinction spectra of oleic acid capped Cu@$Cu_{2-x}O$ NCs incubated with D- (a) and L-cysteine (b) at different pH in 30 °C water bath for 24 h.

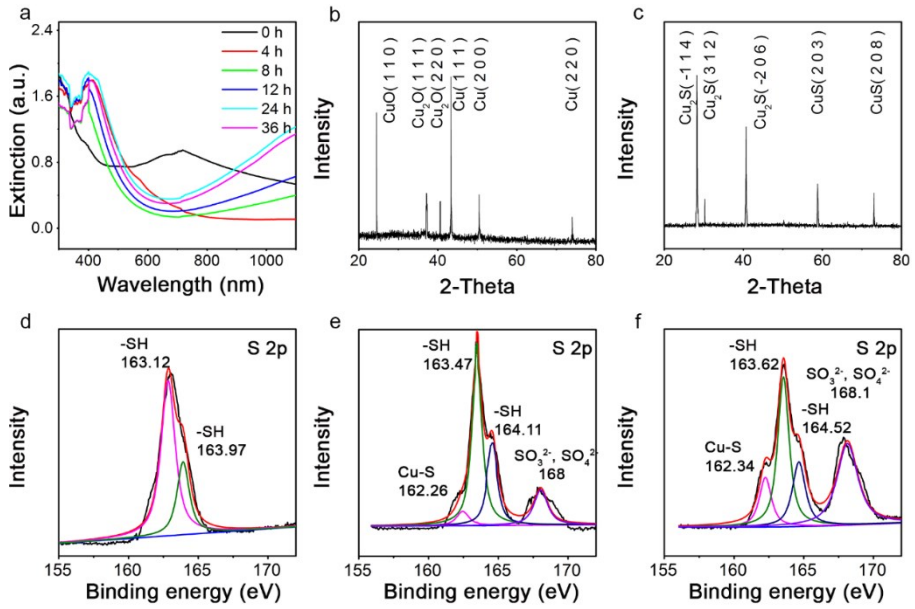

Fig. S5 The evolutions of LSPR bands and structures of the oleic acid capped Cu@$Cu_{2-x}O$ NCs incubated with L-cysteine in 30 °C water bath. (a) The evolution of LSPR extinction spectra of oleic acid capped Cu@$Cu_{2-x}O$ NCs incubated with L-cysteine in 30 °C water bath. XRD patterns of L-cysteine capped Cu@$Cu_{2-x}O$ (b) and L-$Cu_{2-x}S$ (c) NCs. The evolution of XPS spectra of oleic acid capped Cu@$Cu_{2-x}O$ NCs incubated with L-cysteine at different bath time. (d) 0h, (e) 8h, (f) 24h.

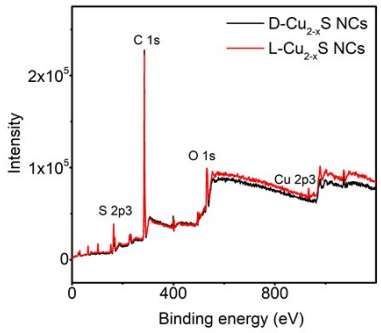

Fig. S6 XPS spectra of D- and L-$Cu_{2-x}S$ NCs.

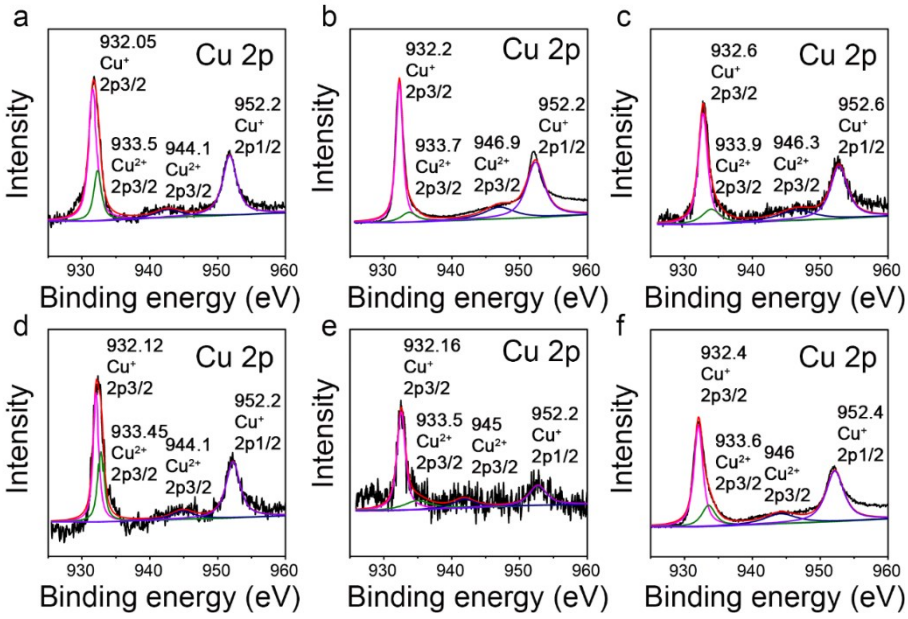

Fig. S7 The evolution of Cu 2p XPS spectra of oleic acid capped Cu@$Cu_{2-x}O$ NCs incubated with D- (a, b, c) and L-cysteine (d, e, f) at different bath time. 0h (a, d), 8h (b, e), 24h (c, f).

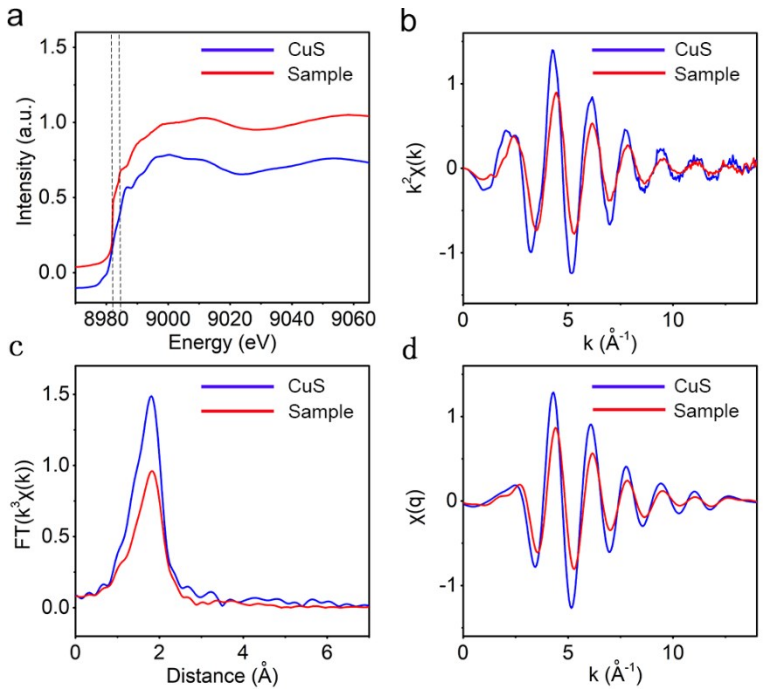

Fig. S8 Cu K-edge XANES (a), k^2-weighted Cu K-edge EXAFS (b), Fourier transformed EXAFS (c) and back-Fourier transformed EXAFS (d) spectra of CuS powder and the sample. Based on (a) (red curve), the energy absorption edges of the sample locate at 8982 and 8984 eV, which correspond to Cu_2S and CuS materials, respectively.[2] Second, according to (b), the k^2-weighted Cu K-edge extended X-ray absorption fine structure (EXAFS) spectra show amplitude of the sample (red curve) is some lower than that of CuS material (black), indicating the less surrounding coordination numbers of the Cu atom of the as-prepared products.[3] Furthermore, the k^2-weighted EXAFS spectra were Fourier transformed to obtain radial structure functions spectra (c). The main peak at 1.8 Å represents bond length of Cu−S in the sample, which exists in both Cu_2S and CuS materials.[2] Then radial structure functions spectra were Fourier back-transformed to obtain EXAFS spectra of the first coordination layer (d).

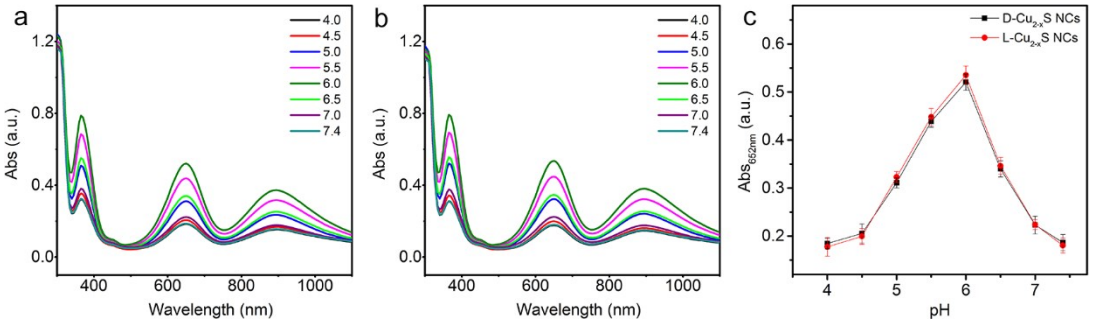

Fig. S9 The effects of pH on peroxidase activity of the D- (a) and L-$Cu_{2-x}S$ (b) NCs. The concentrations of the $Cu_{2-x}S$ NCs, TMB, H_2O_2, are 20 μg mL^{-1}, 0.50 mM, 10 mM, respectively.

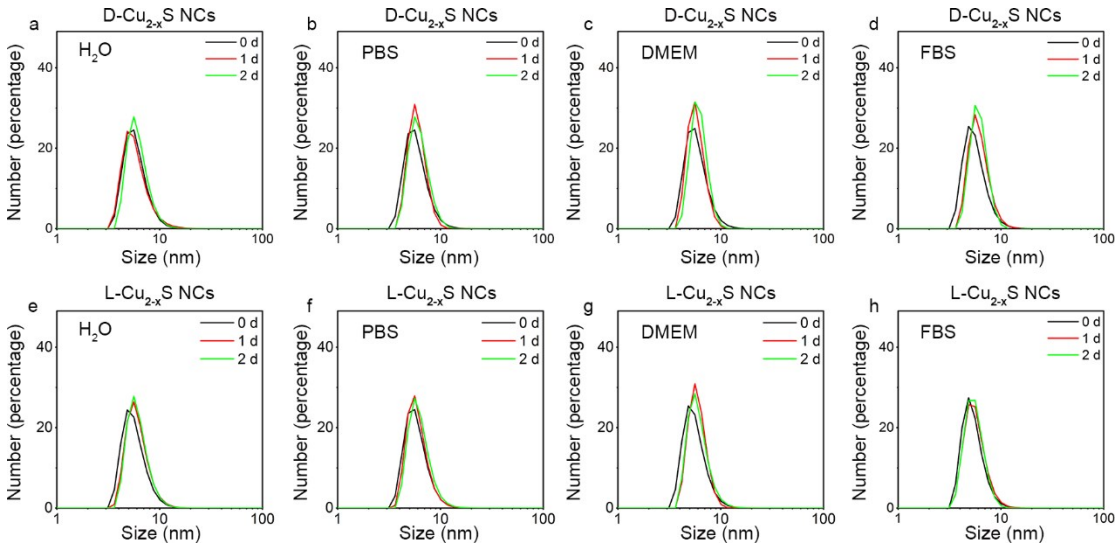

Fig. S10 DLS analysis of the D-$Cu_{2-x}S$ (a, b, c, d) and L-$Cu_{2-x}S$ (e, f, g, h) NCs in H_2O, PBS, DMEM and FBS.

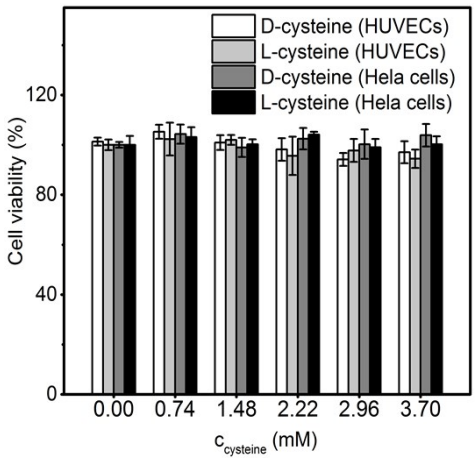

Fig. S11 The viabilities of HUVECs and HeLa cells incubated with D- and L-cysteine for 24 h.

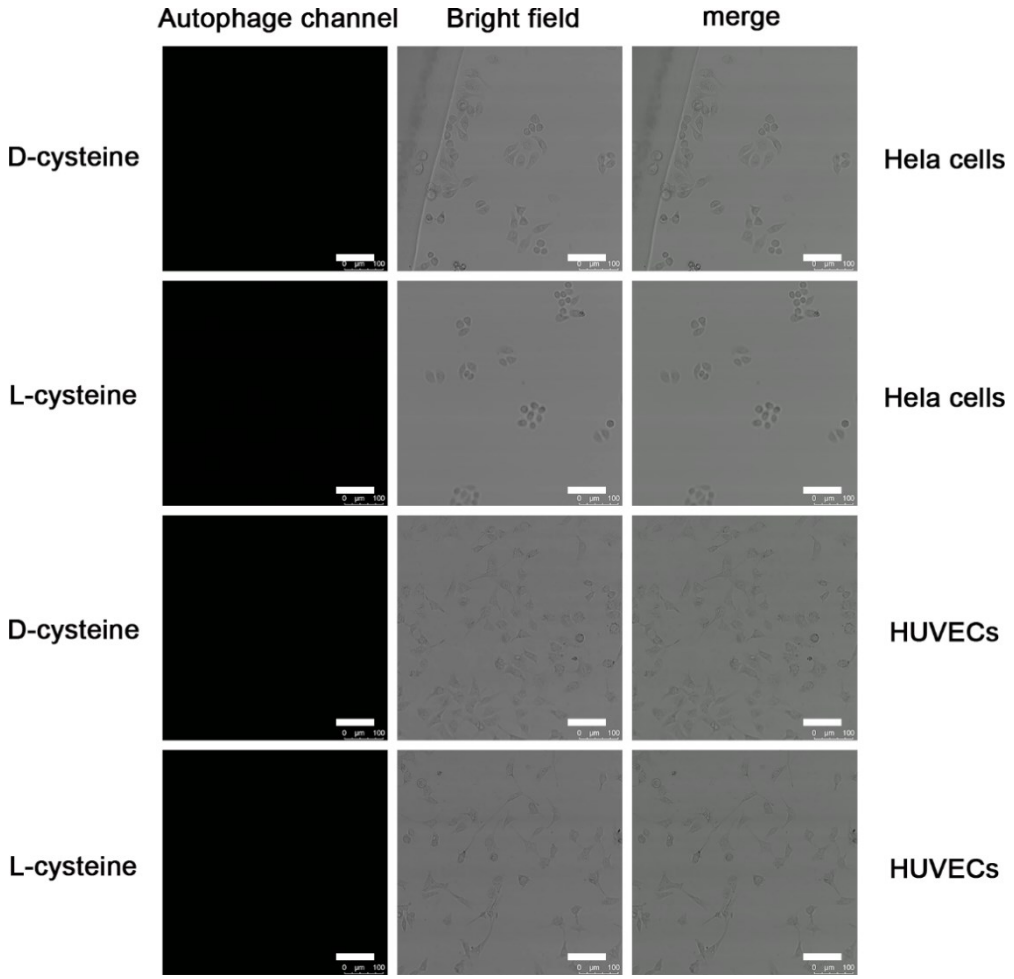

Fig. S12 Autophagy states of HUVECs and HeLa cells incubated with D- and L-cysteine at 1.48 mM, scale bar is 100 μm.

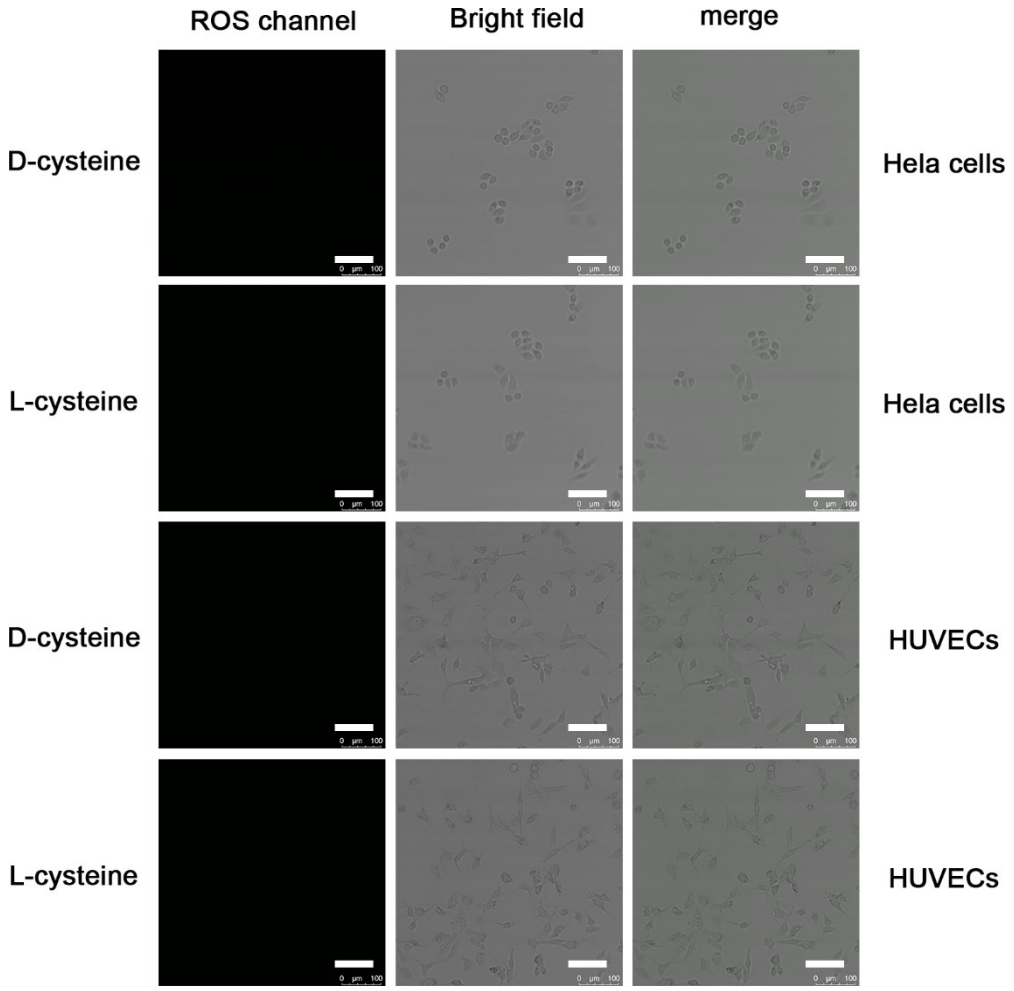

Fig. S13 ROS states of HUVECs and HeLa cells incubated with D- and L-cysteine at 1.48 mM, scale bar is 100 μm.

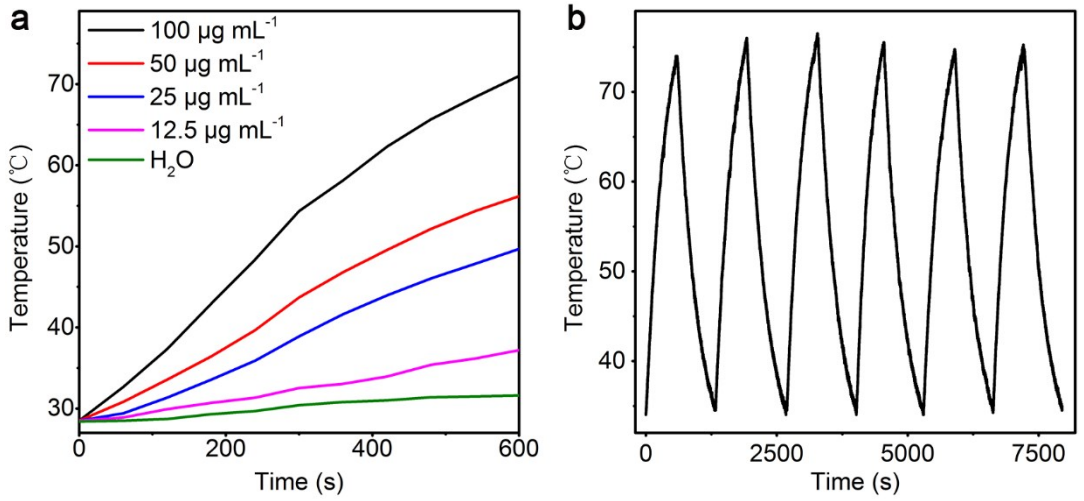

Fig. S14 (a) Concentration dependent photothermal effects of L-$Cu_{2-x}S$ NCs. (b) Temperature changes of L-$Cu_{2-x}S$ NCs at 100 μg mL^{-1} over 6 cycles of laser irradiation/cooling.

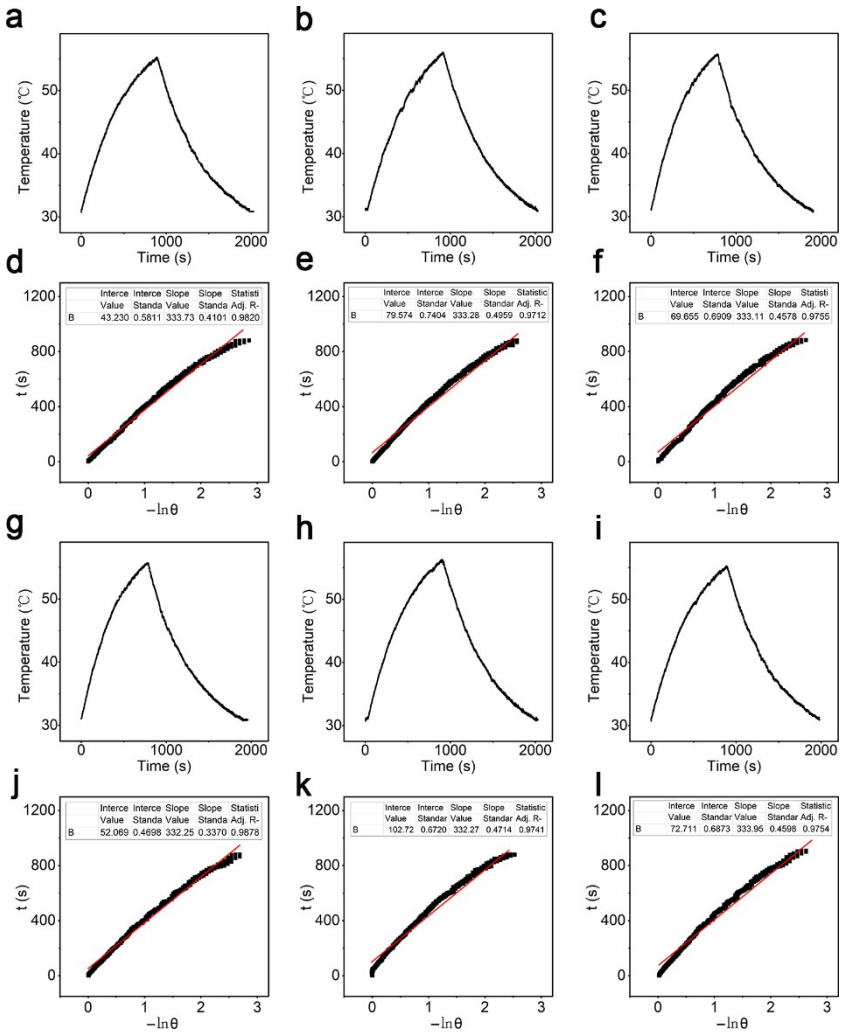

Fig. S15 Three experiments of photothermal effects of D- (a, b, c) and L-$Cu_{2-x}S$ (g, h, i) NCs at 50 μg mL^{-1} under 808 nm laser irradiation for 10 min and cooling process. The linear relationships between cooling time and −ln θ of D-$Cu_{2-x}S$ (d, e, f) and L-$Cu_{2-x}S$ (j, k, l) NCs during cooling process.

The photothermal conversion efficiencies (η) were calculated using following equations.[4]

$$\eta = hS(T_{max,NCs} - T_{max,solvent}) / [I(1-10^{-A_{808}})] \quad (1)$$

$$\tau_s = m_D c_D / (hS) \quad (2)$$

$$t = -\tau_s \ln\theta \quad (3)$$

$$\theta = (T - T_{surr}) / (T_{max,NCs} - T_{surr}) \quad (4)$$

D-$Cu_{2-x}S$ NCs:

① $\eta = mc(T_{max,NCs} - T_{max,H_2O})/[I(1-10^{-A_{808}})\tau_s]$

$= 1\times4.2\times(56.1-31)/[0.75\times(1-10^{-0.477})\times333.73]\times100\%$

$= 62.94\ \%$

② $\eta = mc(T_{max,NCs} - T_{max,H_2O})/[I(1-10^{-A_{808}})\tau_s]$

$= 1\times4.2\times(56-31.2)/[0.75\times(1-10^{-0.477})\times333.288]\times100\%$

$= 63.02\ \%$

③ $\eta = mc(T_{max,NCs} - T_{max,H_2O})/[I(1-10^{-A_{808}})\tau_s]$

$= 1\times4.2\times(56.2-31.1)/[0.75\times(1-10^{-0.477})\times333.11]\times100\%$

$= 63.06\ \%$

L-$Cu_{2-x}S$ NCs:

① $\eta = mc(T_{max,NCs} - T_{max,H_2O})/[I(1-10^{-A_{808}})\tau_s]$

$= 1\times4.2\times(56.3-31)/[0.75\times(1-10^{-0.480})\times332.25]\times100\%$

$= 63.75\ \%$

② $\eta = mc(T_{max,NCs} - T_{max,H_2O})/[I(1-10^{-A_{808}})\tau_s]$

$= 1\times4.2\times(56.1-31.3)/[0.75\times(1-10^{-0.480})\times332.27]\times100\%$

$= 63.56\ \%$

③ $\eta = mc(T_{max,NCs} - T_{max,H_2O})/[I(1-10^{-A_{808}})\tau_s]$

$= 1\times4.2\times(56.2-31.1)/[0.75\times(1-10^{-0.480})\times333.95]\times100\%$

$= 63.43\ \%$

h (mW m^{-2} °C^{-1}): Heat transfer coefficient;
S (m^2): Surface area of the container;
T_{max} (°C): Equilibrium temperature;
T_{surr} (°C): Ambient temperature of the surrounding;
I: The incident laser power density;
A_{808}: The absorbance of $Cu_{2-x}S$ NCs (50 μg mL^{-1}) at 808 nm.

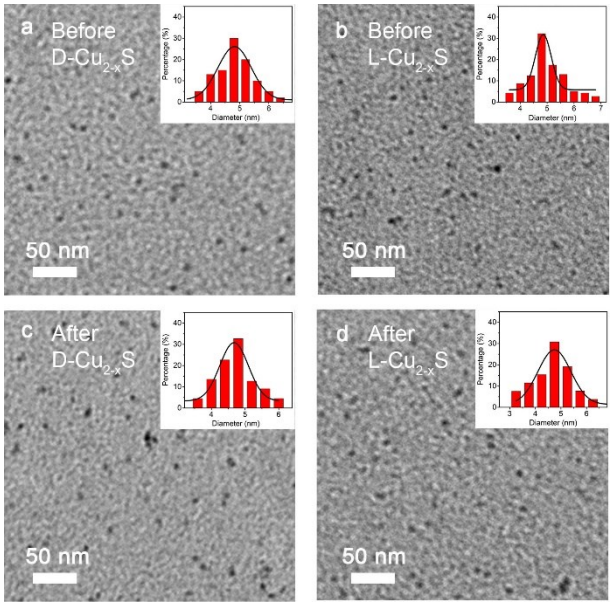

Fig. S16 TEM images of the D- (a) and L-$Cu_{2-x}S$ (b) NCs before 6 cycles of the heating/cooling processes. TEM images of the D- (c) and L-$Cu_{2-x}S$ (d) NCs after 6 cycles of the heating/cooling processes.

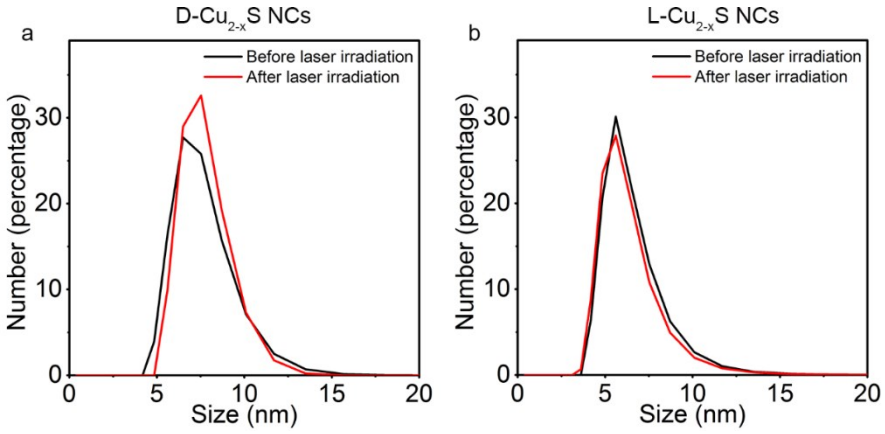

Fig. S17 DLS analysis of D-$Cu_{2-x}S$ (a) and L-$Cu_{2-x}S$ (b) NCs before and after 808 nm laser irradiation.

Table S1 XPS analysis of D- (a) and L-$Cu_{2-x}S$ (b) NCs.

(a)

Type	Start BE	Peak BE	End BE	Atomic %
C1s	295.86	284.8	275.96	81.71
Cu2p	970.86	932.6	925.96	2.3
O1s	545.86	531.57	525.96	8.52
S2p	175.86	163.51	155.96	7.47

(b)

Type	Start BE	Peak BE	End BE	Atomic %
C1s	296.01	284.8	276.11	79.2
Cu2p	971.01	932.75	926.11	2.6
O1s	546.01	531.62	526.11	9.75
S2p	176.01	163.58	156.11	8.45

Table S2 The evolution of Cu 2p XPS spectra analysis of oleic acid capped $Cu@Cu_{2-x}O$ NCs incubated with D- and L-cysteine at different bath time.

Type	bath time	Cu^{+}/Cu^{2+}	Composition
D-NCs	0h	1.50	$Cu_{1.42}O$
D-NCs	8h	1.82	$Cu_{1.47}S$
D-NCs	24h	1.60	$Cu_{1.45}S$
L-NCs	0h	1.48	$Cu_{1.42}O$
L-NCs	8h	1.80	$Cu_{1.47}S$
L-NCs	24h	1.57	$Cu_{1.45}S$

Table S3 Photothermal conversion efficiencies of the three experiments of the D- and L-$Cu_{2-x}S$ NCs at 50 μg mL^{-1}.

Type	1 (%)	2 (%)	3 (%)	Mean (%)	Standard Deviation (%)
D-$Cu_{2-x}S$	62.94	63.02	63.06	63.01	0.0611
L-$Cu_{2-x}S$	63.75	63.56	63.43	63.58	0.1609

3. References

1 M. Yin, C. K. Wu, Y. Lou, C. Burda, J. T. Koberstein, Y. Zhu and S. O'Brien, *J. Am. Chem. Soc.* 2005, **127**, 9506–9511.

2 J. Liu, Y. Zhao, J. Liu, S. Wang, Y. Cheng, M. Ji, Y. Zhou, M. Xu, W. Hao and J. Zhang, *Sci. China Mater.* 2015, **58**, 693–703.

3 J. E. Penner-Hahn, *Coord. Chem. Rev.* 1999, **190**, 1101–1123.

4 D. K. Roper, W. Ahn and M. Hoepfner, *J. Phys. Chem. C* 2007, **111**, 3636–3641.